doi:10.3788/gzxb20154405.0501001

用瑞利激光雷达 16 年观测数据分析合肥地区大气密度分布特征

陈峰[1,2],时东锋[1],黄见[1],苑克娥[1],曹开法[1],胡顺星[1]

(1 中国科学院安徽光学精密机械研究所 中国科学院大气成分与光学重点实验室,合肥 230031)

(2 中国科学院大学,北京 100049)

摘 要:介绍了 L625 瑞利激光雷达系统结构以及基于瑞利散射理论探测大气分子数密度的原理.提出了反复迭代修正大气透过率的计算方法,并通过模拟仿真验证了该算法的可靠性.通过误差分析得到影响大气分子密度不确定度的主要因素为回波信号信噪比以及参考点处大气分子数密度值,给出了回波信号误差产生的主要来源以及参考点选取方法.最后,分析了激光雷达 16 年观测数据反演的结果,得到合肥地区大气分子数密度的月份以及年份分布状况,结果表明:中层大气分子数密度分布呈现明显的季节性分布特征,冬季分布稀疏,夏季分布密集,随年份分布则较为平稳.通过将统计平均得到的密度廓线与 1976 美国标准大气模式比对分析,发现由激光雷达观测反演得到的结果较模式值大,二者的比值在 1.05～1.13 之间.

关键词:大气光学;大气密度分布;瑞利激光雷达;迭代算法;模拟分析

中图分类号:P412.291 **文献标识码**:A **文章编号**:1004-4213(2015)05-0501001-6

Analysis on Molecular Number Density Distribution in the Middle Atmosphere with 16 Years′ Lidar Data in Hefei

CHEN Feng[1,2], SHI Dong-feng[1], HUANG Jian[1], YUAN Ke-e[1], CAO Kai-fa[1], HU Shun-xing[1]

(1 *Key Laboratory of Atmospheric Composition and Optical Radiation, Anhui Institute of Optics and Fine Mechanics, Chinese Academy of Sciences, Hefei* 230031, *China*)

(2 *University of Chinese Academy of Sciences, Beijing* 100039, *China*)

Abstract: The structure of L625 Rayleigh lidar system, principles of atmospheric density measurement which is based on the Rayleigh scattering theory and iterative method to retrieve middle atmosphere density profiles were described respectively. In order to prove the effectiveness of iterative algorithm, simulation analysis was made. Error analysis indicated that contributions to the uncertainty of the retrieved molecular number density mainly derived from signal to noise ratio of the return signals and molecular number density at the reference point. Meanwhile, main error sources of the return signals and method to determine the reference point were given. Finally, according to 16 years' routine observations of L625 Rayleigh lidar, monthly distribution and annual average of molecular number density from 1997 to 2004 and 2006 to 2012 in the middle atmosphere were presented. Results show that molecule number density distribution is sparse in winter and it becomes thick in summer. The yearly distribution of

Foundation item: The Major Program of the National Natural Science Foundation of China(No. 41127901); The National Natural Science Foundation of China (Nos. 41475001,11404344); Knowledge Innovation Program of the Chinese Academy of Sciences(No. KJCX2-EW-N07)

First author: CHEN Feng(1989－), male, M. S. degree candidate, mainly focuses on atmosphere measurement technology with lidar. Email:fengchen0103@126.com

Responsible author(Corresponding author): HU Shun-xing(1966－), male, professor, Ph. D. degree, mainly focuses on atmospheric measurement methodology and technology with diverse lidar systems. Email:sxhu@aiofm.ac.cn

Received: Dec. 2, 2014; **Accepted**: Feb. 3, 2015

molecular number density seems to be relatively stable. Comparison with the model density which is obtained from 1976 USA standard atmospheric model indicates that density ratio profile of L625 Rayleigh lidar to the model density fluctuates between 1.05 and 1.13.

Key words: Atmospheric optics; Molecular number density distribution; Rayleigh Lidar; Iterative method; Simulation analysis

OCIS Codes: 010.1290; 010.1280; 010.3640

0 Introduction

The middle atmosphere has received increasing attention during the past years, especially when climatic change has become so critical[1]. Atmosphere density is one of the important parameters in meteorology, which plays an important role in studying the dynamic and thermo-dynamic properties of the middle atmosphere.

Currently, primary methods to study atmosphere density in the middle atmosphere include satellite-borne instruments[2-4] and ground based Rayleigh lidars. Although satellite-borne instruments are nearly global in coverage, poor vertical resolution characteristic of the passive remote sensing determines that they can't provide the best vertical resolution and accuracy for middle atmosphere density study. Ground based Rayleigh lidar has been widely used when the first density profiles were derived from Rayleigh lidar measurements in 1980[5]. Since that time, shibata et al.[6], Sica et al.[7], Thayer et al.[8] have made studies of middle atmosphere density with ground-based Rayleigh lidar, but few reports, characterize long-term (a decade and more) changes in the middle atmosphere density distribution.

L625 Rayleigh lidar was installed in Hefei (32.0° N, 117.0° E) in 1996, and a great deal of observed data has been obtained since that time. In this paper, we firstly introduce the L625 Rayleigh lidar system, then method to retrieve middle atmosphere density profiles and methodology for error analysis are presented. Finally, we characterize the main characteristics of middle atmosphere density distribution in Hefei ranging from 25 km to 60 km and reveal the comparative results with 1976 USA standard atmospheric model.

1 L625 Rayleigh lidar system

L625 Rayleigh lidar system is shown in Fig. 1 and the following paragraphs describe the system configuration in detail. Table 1 lists the main characteristics of L625 Rayleigh lidar system.

The laser transmitter is a frequency tripled Nd : YAG pulse laser at 532 nm, whose monitored average output energy is 100 mJ/pulse and the repetition frequency is 10 Hz. To make sure that the transmitted beams are directed vertically into the atmosphere, two

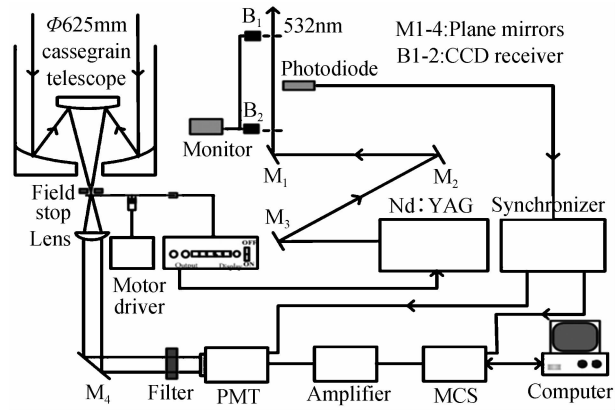

Fig. 1 L625 Rayleigh lidar system configuration

Table 1 The characteristics of L625 Rayleigh lidar system

Transmitter	
Laser	Nd : YAG
Wavelength	532 nm
Energy per pulse	100 mJ
Pulse duration	18 ns
Pulse repetition rate	10 Hz
Beam divergence	≤1 mrad
Receiver	
Telescope	625 mm cassegrain
Field of view	2 mrad
Photomultiplier	9214QB
PMT quantum efficiency	0.12
Filter FWHM	1 nm
Photon counter	
Photon counter	
Vertical resolution	150 m
Channel number	800
Laser shots	12 500
Preamplifier	VT120B(gain:200)

baffles with a round hole punched in the center point are installed on the vertical position with 12 meters away from each other. Those baffles' position was carefully adjusted so that the connection between two baffles' center point is parallel to the telescope axis. Two CCD receivers are installed on the side of the baffles, which are used to monitor the transmitted beams. Modulating the mirror system installed along the light path until the transmitted beams can pass through the round holes.

The backscattered light is received by a Cassegrain telescope whose field of view is 2 mrad and the diameter is 625 mm. Just below the focus of the

telescope is a mechanical chopper, which blocks the intense low-altitude returns from the detection system. The mechanical chopper wheel consists of two blades on opposite sides and rotates at a rate of 800 Hz. The diameter of this mechanical chopper wheel is 92 mm. The chopper blade position is monitored by a photodiode. Output modulated signal of the photodiode is divided into a 10 Hz pulse signal which is used to trigger the laser *Q*-switch by a frequency distribution device. The output laser beams are monitored by a photodiode installed on the side of the transmitted beams. Signals from the photodiode are used to trigger (Photomultiplier Tube, PMT) and data acquisition device.

After passing through the mechanical chopper, the collected light is collimated by an objective lens and directed by a reflected mirror. The light then passes through the narrowband interference filter and is received by a Cooled(−20 ℃) PMT. The output signal of the PMT is firstly amplified and then sent to the data acquisition device (multichannel scaler). The multichannel scaler provides gated sampling of the lidar signal with dwell time selectable from 100 ns to 1 300 s per channel and count rates up to 150 MHz.

2 Method

2.1 Lidar equation

Lidar equation[4] for the signal-scattering can be expressed as

$$P(R) = P_{\mathrm{L}} \frac{C_{\mathrm{T}}\beta(R)}{R^2}\exp\left[-2\int_0^R \alpha(r)\mathrm{d}r\right] \tag{1}$$

where $P(R)$ is the received power from distance R; P_{L} is the output laser power; C_{T} is a const which is the product of the telescope receiver area, the collection and detection efficiency; $\beta(R)$ and $\alpha(R)$ are the volume backscatter and extinction coefficient by atmosphere gasses and aerosol particles, respectively.

2.2 Principle of the Measurement

Basic assumptions to measure middle atmosphere density with the Rayleigh scattering theory include the following three items. Firstly, only the molecular contributions to the return signals are considered above the height of 25 km and the aerosol scatterers can be ignored[9-10]. Secondly, molecular number density at the reference point is a known value. Thirdly, Rayleigh backscattering cross section is independent of altitude[11]. Thus, atmosphere density above 25 km can be expressed as

$$N(R) = \frac{P(\lambda,R)n(R_0)R^2}{P(\lambda,R_0)R_0^2}Q^2(\lambda,R_0,R) \tag{2}$$

$$Q(\lambda,R_0,R) = \exp\left[\int_{R_0}^R \alpha(\lambda,R)\mathrm{d}r\right] \tag{3}$$

where $n(R_0)$ is atmosphere density at the reference height R_0, which can be obtained from the standard atmospheric model. $P(\lambda,R)$ represents the return signal at the wavelength λ and the distance R. The background noise has been subtracted already. $Q(\lambda,R_0,R)$ represents atmospheric transmission between altitude R_0 and R. $\alpha(\lambda,R)$ represents the volume atmosphere extinction coefficient at the wavelength λ, which can be obtained from the following expressions[12].

$$\alpha(\lambda,R) = S_m\beta(\lambda,R) \tag{4}$$

$$\beta(\lambda,R) = 5.45\times N(R)[\lambda/550]^{-4}\times 10^{-28} \tag{5}$$

where $\beta(\lambda,R)$ is the volume atmosphere backscattering coefficient and it can be regarded as the product of molecular number density and the Rayleigh scattering section at scattering angle $\theta=\pi$. S_m is the extinction to backscatter ratio or lidar ratio for the molecular scattering and is usually approximated as $8\pi/3$.

Atmospheric transmission $Q(\lambda,R_0,R)$ is unknown and cannot be obtained precisely, so iterative method is taken into account to lower its effect for the final result. This iterative method consists of three steps. In the first step, $Q(\lambda,R_0,R)=1$[13] is assumed for all heights above 25 km. The second step is to calculate the molecular number density from Eqs. (2). In the third step, we can obtain atmospheric transmittance from the Eqs. (3)～(5) mentioned above and the value calculated in the second step. Repeat step 2 and 3 described above until the relative deviation of atmospheric transmittance between the former and the latter is less than 1%. Generally, this iterative process will be terminated after 2 or 3 repetitions.

2.3 Simulation analysis

To make sure this iterative method is effective, simulation analysis is made. Usually, it is hard to get the simulated return signals from the lidar equation because of the difficulty of obtaining the precise overlap factor, aerosol extinction and backscattering profiles. Under this circumstance, Eq. (6) will be a way to get the simulated return signals, because the aerosol contributions to the return signals profile can be neglected above 25 km, overlap factor equals to 1 and the volume atmosphere backscatter and extinction coefficient can be obtained from Eqs. (4), (5) via the atmospheric model data. We just need to assume the return power $P(\lambda,R_0)$ at the distance R_0 which is usually at the upper boundary altitude.

$$P(\lambda,R) = \frac{P(\lambda,R_0)N(R)R_0^2}{n(R_0)R^2}Q^2(\lambda,R,R_0) \tag{6}$$

Fig. 2 presents the retrieved density profile using the simulated return signals with iterative method. Fig. 3 presents the density ratio profile of the retrieved density to 1976 USA standard atmospheric model.

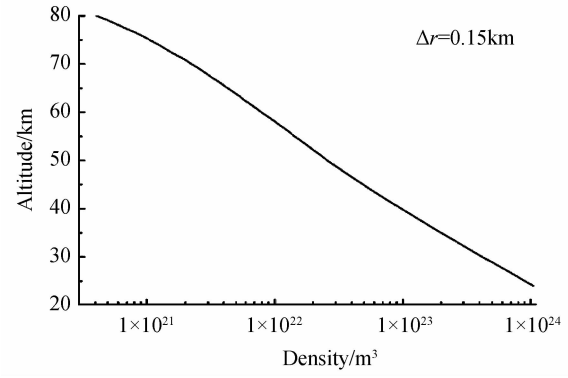

Fig. 2 Retrieved density profile

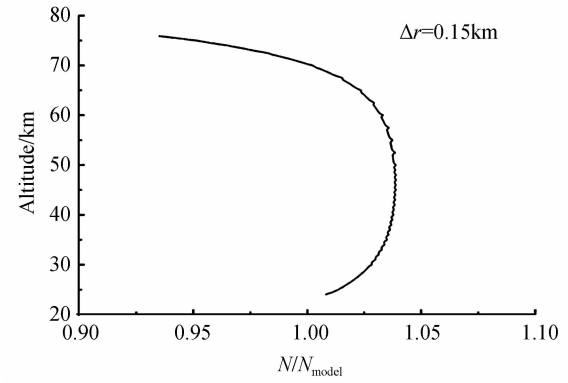

Fig. 3 Density ratio profile of the retrieved density to 1976 USA standard atmospheric model

It is evident that this iterative method is an effective way to retrieve the molecular number density profile. The density ratio profile of the retrieved density to 1976 USA standard atmospheric model fluctuates between 0.95 and 1.05 mostly. The main reason for those differences may come from the simulated return signals which result from the volume atmosphere backscatter and extinction coefficient.

3 Error Analysis

For a function χ, derived from several indirect measurement variables $u, v\cdots$, the uncertainty of this function can be expressed as the following equation[14]

$$(\delta\chi)^2=(\delta u)^2\left(\frac{\partial\chi}{\partial u}\right)^2+(\delta v)^2\left(\frac{\partial\chi}{\partial v}\right)^2+2C_{uv}^2\left(\frac{\partial\chi}{\partial u}\right)\left(\frac{\partial\chi}{\partial v}\right)+\cdots \tag{7}$$

where $\delta u, \delta v$ denote the uncertainty of variable u, v and C_{uv}^2 is the covariance between measured variables u and v. This covariance can be expressed as

$$C_{uv}^2=\lim_{n\to\infty}\frac{1}{n}\sum[(u_i-\bar{u})(v_i-\bar{v})] \tag{8}$$

where $\bar{u}, \bar{v}$ denote the average value of the variable u, v respectively and u_i, v_i represent the values obtained in a particular measurement$i$. The covariance vanishes when error $(u_i-\bar{u})$ are uncorrelated with the error $(v_i-\bar{v})$. Supposing that both of the uncertainty of absolute altitude R and R_0 can be neglected and since the relative deviation of atmospheric transmittance between the former and the latter is less than 1%, we can also ignore the uncertainty of atmospheric transmittance . For purposes of error analysis and also to simplify computation, it is necessary to define expression as

$$P(\lambda,R,R_0)=\frac{P(\lambda,R)}{P(\lambda,R_0)} \tag{9}$$

It is obvious that the uncertainty of $P(\lambda,R,R_0)$ will be vanished when $R=R_0$ and $P(\lambda,R), P(\lambda,R_0), n(R_0)$ are not related to each other when $R\neq R_0$. Thus, uncertainty of molecule number density can be expressed as

$$(\sigma N)^2=\begin{cases}\left[\frac{\partial N(R)}{\partial P(\lambda,R)}\right]^2[\delta P(\lambda,R)]^2+\left[\frac{\partial N(R)}{\partial P(\lambda,R_0)}\right]^2[\delta P(\lambda,R_0)]^2+\left[\frac{\partial N(R)}{\partial n(R_0)}\right]^2[\delta n(R_0)]^2 & R\neq R_0\\ \left[\frac{\partial N(R)}{\partial n(R_0)}\right]^2[\delta n(R_0)]^2 & R=R_0\end{cases} \tag{10}$$

Eq. (10) reveals that the total uncertainty of molecular number density mainly includes contributions from the return signals and the molecular number density at the reference height.

Considering that fluctuations of the return photon signals obey the Poisson statistical distribution[15-16], thus estimation error resulting from the fluctuations of photon counting can be expressed as

$$\frac{\delta P(\lambda,R)}{P(\lambda,R)}=\frac{[P(\lambda,R)+n]^{1/2}}{P(\lambda,R)} \tag{11}$$

where n is the background noise which primarily includes viewed background radiation and internal electronic detector noise. Currently inward stepwise integration[17] has been widely used to retrieve density profits, because it can lose its dependence on the atmosphere density at the reference height rapidly and leads to a stable result. Reference height R_0 is determined when $\frac{P(\lambda,R)}{\delta P(\lambda,R)}$ is approximated as 5 by Eq(11).

4 Results and discussion

4.1 Density distribution property

A large number of experiments with L625 Rayleigh lidar have been made since 1996 in Hefei, China. 12 500 laser shots have been accumulated and the total time for each experiment is over one hour in order to obtain reliable result. About 300 groups of day - observation data are chosen from 1997 to 2013.

Basic fundamentals for choosing these data include the following two items. Firstly, the returned signal should have enough resistance to noise, especially over the range of 60 km. Secondly, data files with anomalous inversion results should be excluded.

Statistical analysis on these 300 groups of data is given from two aspects. Firstly, molecule number density distribution ranging from 25 km to 60 km is shown by month. Fig. 4 and 5 present the results from January to December with the altitude from 25 km to 42.5 km and 42.5 km to 60 km, respectively. It is obvious that seasonal variation of molecule number density distribution appears: from March to August, molecule number density increases gradually and it reaches the maximum in August, then it begins to decrease gradually and the minimum appears in February.

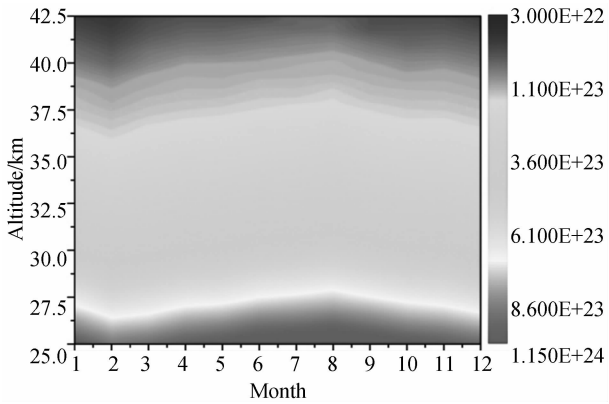

Fig. 4 Molecular number density distribution ranging from 25 km to 42.5 km

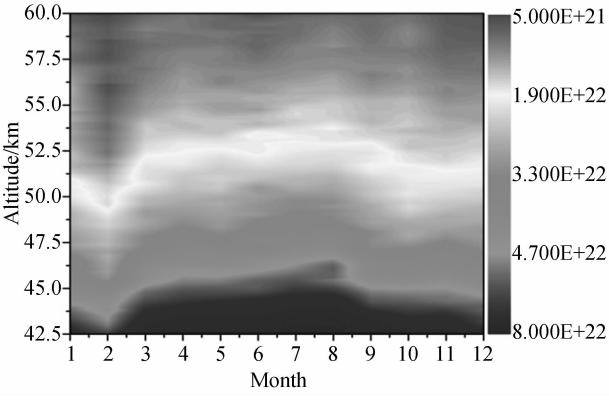

Fig. 5 Molecular number density distribution ranging from 42.5 km to 60 km

Secondly, annual average of molecular number density from 1997 to 2004 and 2006 to 2012 are shown in Fig. 6 and Fig. 7, respectively, and in 2005 L625 lidar system was upgraded so that few experiments are made during that time. According to the Fig. 6 and 7, we can see that distribution of molecular number density seems to be relatively stable as a whole except some fluctuations exist from 45 km to 52 km.

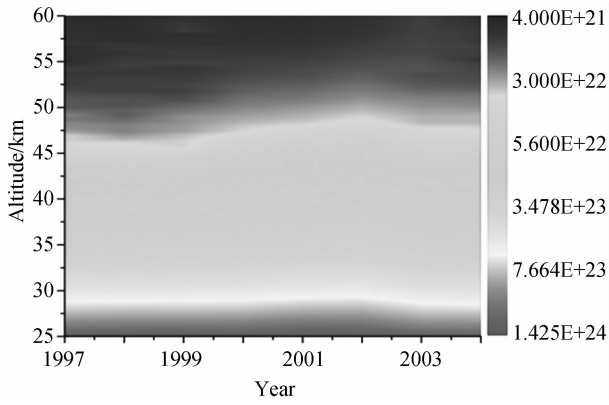

Fig. 6 Molecular number density distribution from 1997 to 2004

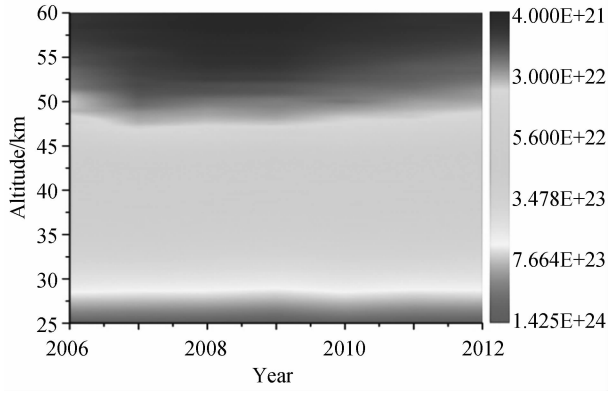

Fig. 7 Molecular number density distribution from 2006 to 2012

4.2 Average density distribution profile

Average molecule number density is obtained by averaging all of the 300 groups of data. Comparative analysis of the result obtained from L625 Rayleigh lidar and that from the 1976 USA standard atmospheric model is shown in Fig. 8 and 9. American standard atmospheric model (USA Standard Atmosphere Model, 1976) is a modified version of the USA 1962 standard atmosphere, which represents idealized and static average mid-latitude atmospheric structure. Analysis shows that: molecule number density obtained from the L625 Raleigh lidar are larger than that from the 1976 USA standard atmospheric model , and the

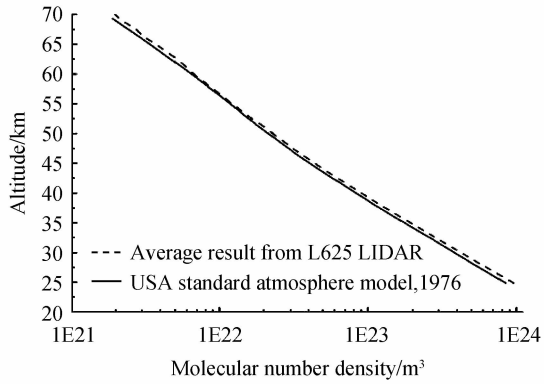

Fig. 8 Molecular number density with log10 scale

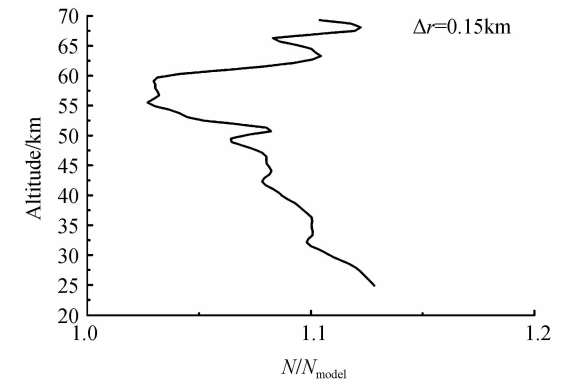

Fig. 9 Density ratio of average result from lidar to 1976 USA Standard Atmospheric model

density ratio profile of L625 lidar to the model density profile fluctuates between 1.05 and 1.13.

5 Conclusions

Molecule number density distribution is obtained from L625 Rayleigh lidar with 16 years′ observational data . Analysis shows that obvious seasonal distribution exists between 25 km to 60 km and molecular number density reaches maximum on summer , minimum on winter. Analysis on annual average molecule number density finds that density distribution is relatively stable as a whole during the 16 years apart from some fluctuations in the stratopause. Meanwhile, results from the comparative analysis show that density ratio of average result from L625 Rayleigh lidar to 1976 USA standard atmospheric model approaches to 1 gradually with the altitude increasing from 25 km to 57 km and then begins to diverge from it.

References

[1] RAMASWAMY V, CHANIN M L, ANGELL J, *et al*. Stratospheric temperature trends: Observations and model simulations[J]. *Reviews of Geophysics*, 2001, **39**(1): 71-122.

[2] BURTON S P, THOMASON L W. Molecular density retrieval and temperature climatology for 40 ~ 60 km from SAGE II[J]. *Journal of Geophysical Research* , 2003, **108**(D19): ACL2. 1-ACL2. 9.

[3] FUNKE B, LÓpez-Puertas M, García-Comas M, *et al*. GRANADA: A generic radiative transfer and Non-LTE population algorithm [J]. *Journal of Quantitative Spectroscopy and Radiative Transfer*, 2012, **113**(14): 1771-1817.

[4] WEITKAMP C. Lidar range-resolve optical remote sensing of the atmosphere[M]. Germany: Springer Science and Business Media, 2005: 6-12.

[5] HAUCHECORNE A, CHANIN M L. Density and temperature profiles obtained by lidar between 35 and 70 km [J]. *Geophysical Research Letters*, 1980, **7**(8): 565-568.

[6] SHIBATA T, KOBUCHI M, MAEDA M. Measurements of density and temperature profiles in the middle atmosphere with a XeF Lidar[J]. *Applied Optics* , 1986, **25**(5): 685-688.

[7] SICA R J, SARGOYTCHEV S, ARGALL P S, *et al*. Lidar measurements taken with a large-aperture liquid mirror. 1. rayleigh-scatter system[J]. *Applied Optics*, 1995, **34**(30): 6925-6936.

[8] THAYER J P, NIELSEN N B, WARREN R E, *et al*. Rayleigh lidar system for middle atmosphere research in the arctic[J]. *Optical Engineering*, 1997, **36**(7): 2045-2061.

[9] WU Yong-hua, HU Huan-ling, ZHOU Jun, *et al*. Distribution of aerosol extinction in the lower troposphere by Micro-pulse lidar observations[J]. *Acta Optica Sinica*, 2000, **14**(4): 503-508.

[10] THIERRY L, PHILIPPE K, SHE C Y, *et al*. Temperature climatology of the middle atmosphere from long-term lidar measurement at middle and low latitudes[J]. *Journal of Geophysical Research*, 1998, **103**(D14): 17191-17204.

[11] BOHREN C F, HUFFMAN D R. Absorption and scattering of light by small particles[M]. Canada: John Wiley & Sons, 2008:382-389.

[12] COLLIS R T H, RUSSELL P B. Lidar measurement of particles and gases by elastic backscattering and differential absorption [M]. New York: Laser monitoring of the atmosphere, 1976: 71-151.

[13] CHEN W N, TSAO C C, NEE J B. Rayleigh lidar temperature measurements in the upper troposphere and lower stratosphere[J]. *Journal of Atmospheric And Solar-Terrestrial Physics*, 2004, **66**(1): 39-49.

[14] RUSSELL B P, SWISSLER T J, MCCORMICK M P, *et al*. Methodology for error analysis and simulation of Lidar aerosol measurements[J]. *Applied Optics*, 1979, **18**(22): 3783-3796.

[15] MEASURES R M. Laser remote sensing: fundamentals and applications[M]. 2nd, ed. New York: Krieger Publishing Company & Malabar, 1992:286-288.

[16] DAVID C, HAEFELE A, KECKHUT P, *et al*. Evaluation of stratospheric ozone, temperature, and aerosol profiles from the LOANA lidar in Antarctica[J]. *Sciverse Sciencedirect*, 2012, **103**(6): 209-225.

[17] FERNALD F G. Analysis of atmospheric lidar observations: some comments[J]. *Applied Optics*, 1984, **23**(5): 652-653.